Robust Pose Invariant Shape-based Hand Recognition

A. El-Sallam, F. Sohel, and M. Bennamoun
School of Computer Science and Software Engineering
The University of Western Australia,
35 Stirling Highway Crawley, WA 6009, Australia
Email: *{elsallam, Ferdous.Sohel, m.bennamoun}@csse.uwa.edu.au*

Abstract— ***This paper presents a novel technique for hand shape and appearance based personal identification and verification. It has two major building blocks. A segmentation block presents robust and fully automatic algorithms which are able to accurately segment the hand's palm and fingers irrespective of colour contrast between the fosreground and background. They achieve a consistent representation of the fingers and the palm regardless of their pose/orientation or the spaces between the fingers. In the feature extraction/matching block, the iterative closest point (ICP) algorithm is employed to align the images. Both shape and appearance based features are extracted and comparatively assessed. The modified Hausdorff distance and independent component analysis (ICA) algorithms are used for shape and appearance analysis. Identification and verification were performed using fusion strategies upon the similarity scores of the fingers and the palm. Experimental results show the proposed system exhibits an accuracy of over 98% in hand recognition and verification in a database consisting of 500 different subjects.***

Keywords- hand shape recognition; image segmentation; biometrics.

I. INTRODUCTION

Recently, there has been increased interest in developing biometrics based verification and identification systems which has led to intensive research in fingerprint, face, hand, ear, iris, and palmprint recognition and authentication [1]. Each biometric has its own strength and weakness depending on the specific application and its requirements. There are several reasons for developing hand-based verification/identification systems. First, the shape of the hand can be easily captured in a relatively user friendly manner by using conventional charge coupled device (CCD) cameras. Second, this technology is more acceptable by the public in daily life mainly because it lacks a close connection to forensic applications. Finally, there has been some interest lately in fusing different biometrics to increase system performance [2]. The ease of use and acceptability of hand-based biometrics make hand shape a good candidate in these heterogeneous systems.

Most of the hand-based biometric schemes in the literature fall into the broad category of geometric features of the hand. For example, Sanchez-Reillo et al. [3] select 25 features, such as finger widths at different latitudes, finger and palm heights, finger deviations and the angles of the interfinger valleys with the horizontal, and model them with Gaussian mixtures. Jain et al. [4] have used a peg-based imaging scheme and obtained 16 features, which include length and width of the fingers, aspect ratio of the palm to fingers, and thickness of the hand. The prototype system they developed was tested in a verification experiment for web access over for a group of ten people [5]. Kumar et al. [6-8] extract geometric features. Öden et al.[9], in addition to geometric features such as finger widths at various positions and palm size, have made use of finger shapes. These shapes have been represented with fourth degree implicit polynomials, and the resulting sixteen features are compared with the Mahalanobis distance. Amayeh et al. [1] uses high order Zernike moments.

In this paper, we propose a novel, peg-free approach to hand based verification and identification which is not sensitive to hand and finger pose and the colour contrast to the background. First, we propose a novel hand palm and fingers segmentation algorithm that is robust, scale and aspect ratio invariant. It is invariant to the hand and/or the finger(s) pose and/or orientation. To segment the hand from the background, we propose an adaptive thresholding algorithm combined with a skin colour detector. This is followed by a number of image processing steps (e.g., image morphing) to remove isolated pixels and fill the holes in the segmented hand. Once this is achieved, we then use the skeleton and the contour of the segmented hand to estimate its global pose and the individual pose of each finger whereupon the palm and each finger are separated and represented in a pre-defined and consistent orientation and representation. Several studies have shown that peg-based alignments are not very satisfactory and can in some cases represent a considerable source of failure. To reduce user inconvenience, peg removal is considered but this brought more challenging research factors due to the increase in intra-class variance. This has been reported as critical problem since high-order Zernike moments are sensitive to small changes in silhouette shape [3]. Besides it is a peg-free, our algorithm, has several advantages when compared with the existing ones, (i) the arm or any object attached to it (e.g., clothes, watches) does not have any effect in our algorithm, (ii) unlike [1], our algorithm does not require any initialization (e.g., palm radius), (iii) it is fast since it does not involve an iterative nature, (iv) in-between finger points are easy to extract using our algorithm and we use them to exclude the arm portion and classify if the hand is a right or a left one, (v) current methods assume that the maximum pose angle of the hand is less than 45 degrees. However, our algorithm can efficiently handle any pose, (vi) to extract each finger, our algorithm does not use connected component analysis but a simple mathematical rotation method. Finally, to improve verification and identification accuracy and robustness, we fuse information from different parts of the hand (e.g., fingers and the palm).

This research was supported by a UWA Research Development Award, a UWA Postdoctoral Fellowship, and an ARC discovery projects (DP0771294 and DP110102166).

978-1-4244-8756-1/11/$26.00 ©2011 IEEE

Various features have been used in biometric based hand recognition: Gabor filters, line features and principal component analysis (PCA) in [8], Zernike moments in [1], Hausdorff distance and independent component analysis (ICA) in [10]. Fusing information from different biometric modalities (i.e., face, fingerprint, hand) has received considerable attention lately. However, fusing information from different parts of the same biometric has been considered to a lesser extent. For example, Kumar and Zhang [7] have investigated feature selection of hand shape and palm print features. Cheung et al. [11] have proposed a two-level fusion strategy for multimodal biometric verification, Amayeh et al. [1] is mostly related to component-based approaches in object detection and recognition. Our approach uses a two-level fusion strategy for multimodal biometrics. The first level of fusion considers shape and appearance scores separately while the second level fuses the score of the first fusion level.

The rest of the paper is organized as follows: An overview of the proposed system is presented in Section 2. Section 3 describes our hand image segmentation and pose-correction algorithms. Section 4 presents the various feature extraction, fusion and matching techniques. Experimental results and analysis are presented in Section 5 with some concluding remarks drawn in Section 6.

II. THE OVERALL SYSTEM

The proposed hand based identification and authentication system consists of four major modules (see Figure 1): (i) segmentation of fingers and palm and pose correction, (ii) feature extraction, (iii) fusion of features and score level data, (iv) matching: recognition and verification.

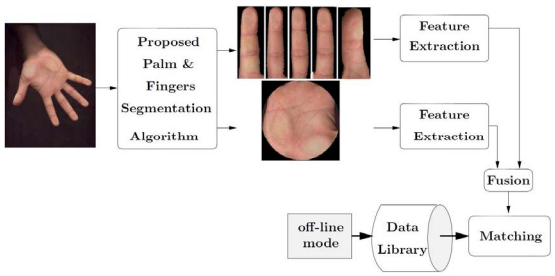

Figure 1: Proposed robust pose invariant shape-based hand recognition system.

A detailed description of these modules is presented in the following sections. The system operation can be divided into an offline enrolment, and online authentication and identification phases. During the offline enrolment phase, the various biometrics of individuals are acquired. Features are then extracted from the biometrics and fused within the same representation. The unified feature representations are then recorded in a database. During the online phase, the relevant multiple biometrics of an individual are acquired and fused in a unified representation consistent with the recorded database which is then matched with the biometric representations that are stored in the database. The decision making module then makes a decision based on the matching score(s).

III. HAND SEGMENTATION, POSE ESTIMATION AND CORRECTION

This algorithm has a number of steps which are briefly described as follows.

Step 0:

- To segment the hand from the background, we developed a background segmentation algorithm that combines a global image threshold using Otsu's method and a skin colour detector.

Step 1:

- The skeleton of the hand's binary image is then determined using the technique proposed in [12].
- Then the centre of mass (CoM) point of the hand skeleton is found (green circle)
- We proposed an edge detection algorithm to extract the corner points of the hand skeleton (green stars).

Step 2:

- The skeleton of the negative of the background binary image is obtained and its corner points are extracted (cyan stars).

Step 3:

- The in-between finger points (cyan stars with a red circle) are identified as four points amongst the corner points (in the background skeleton) which are the nearest to the CoM point and are located at the maximum tip of the skeleton sharp edges.
- The identification of these four in-between finger points is robust and reputable for any hand with any pose and orientation as long as the background has no skin colour-like subject.

Step 4:

- To search for the finger tips, three points are identified (as seen in Figure 2 Step 4) from the four in-between finger points obtained above in Step 3,
- The three points are then used to determine whether the hand is a right or a left one. This is done by comparing the location of the fourth point which is near to the thumb with respect to these three points.
- The middle point of these three points is found and two lines (cyan) are used to classify and isolate the finger tip points (green stars with yellow circles) from all other hand skeleton points (green stars).
- The side where the two lines make the larger angle represents the area of interest for finger tips identification.
- This area of interest excludes the arm and any object (e.g. clothes) attached to it, making our algorithm robust.

Step 5:

- The finger tips and the in-between finger points are now identified but due to the skeletonising operation which includes filtering using a Gaussian point spread function, the points need to be accurate.

Step 6:

- All points obtained in Step 5, are corrected by finding the intersecting points between the hand contour and the skeleton lines carrying the identified points (in Step 5).

Step 7:

- The final identified points of the finger tips and the in-between finger points are determined.

Step 8:

- To estimate the global pose of the hand, the three in-between finger points (shown in Figure 2 Step 8) are used. The point between the thumb the index finger is excluded.
- Two lines from the middle point (the point between Middle and Ring fingers) and the other two neighbouring points are then created.

- The centres of the above two lines are then determined and two perpendicular lines (white) to those lines starting from their two centres are created.
- The intersecting point between the two white lines created above is found.
- The line that passes through the above intersecting point and middle point (between Middle and Ring fingers) represents the global pose of the hand.
- The pose angle of the hand is then calculated.

Step 9:

- Using this pose angle, the hand pose/orientation is corrected.
- Finger tips and in-between finger points are then rotated by the same angle.
- Using the in-between finger points, the midpoint of each finger is determined.
- The pose of each finger is then estimated using the line passes through the finger tip and the finger midpoint.

Final results:

- Using the in-between finger points, finger tips and the finger pose; each finger is cropped and reoriented in a vertical form in a pre-defined image size that is consistent for all hands.
- The hand palm is also cropped by fitting a circle/disc to the in-between finger points and the finger midpoints. For consistency and to overcome any scaling problem, the cropped palm is resized to fit a pre-defined radius of a circle.
- Through testing, it has been concluded that finger movements do not change, the location of the in-between finger points significantly. This gives the in-between finger points the advantages of being reliable information for a scale invariant palm print verification since all palms are resized to a pre-defined disc of a known size that is based on these points.

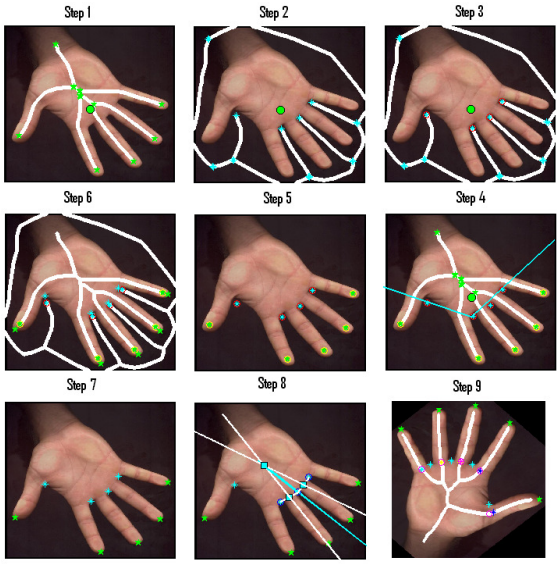

Figure 2: Steps of the proposed hand's palm and fingers segmentation, pose estimation and correction algorithm (picture best seen in colour).

IV. Feature Extraction and Feature Matching Strategies

Once the fingers and the palm images are segmented and their pose are corrected, various shape and appearance based features are extracted. The palm and each finger of the hand were considered separately for feature extraction. The overall feature extraction and feature matching strategy is shown in Figure 3. In the shape based feature recognition method, the test finger or the palm is passed through the iterative closest point algorithm (ICP) [13] for alignment with the corresponding training finger/palm model before the geometric distance is measured using the modified Hausdorff distance technique. This distance represents the similarity score of the finger (or palm). Similarity scores of the different fingers and the palm are then fused together in Fusion 1 using a weighted sum approach which was used in [14]. In the appearance based method we use the ICA technique so that the statistically independent shape features are extracted from the training dataset. These independent features are then applied to the test data. The minimum Euclidean distance between the features are considered the similarity score. These steps are repeated for all five fingers and the data are fused together using the weighted sum approach (described in Section IV.C) in the first level of fusion (Fusion 2). Scores of both Fusion 1 and Fusion 2 are then fused together using the *mean* rule to obtain the final score of finger recognition (Fusion 3). A brief description of the various feature extraction and fusion techniques used in this paper is given below:

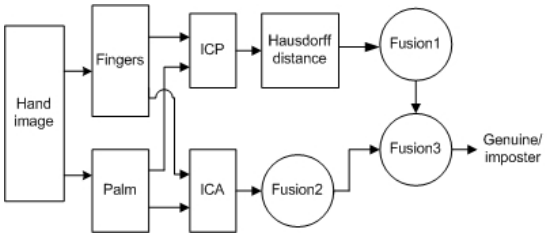

Figure 3: A schematic diagram for feature extraction and feature matching.

A. Modified Hausdorff Distance

In order to compare different shape geometries the Hausdorff distance is a very efficient method. This metric has been extensively used in binary image comparison and computer vision [15]. The advantage of Hausdorff distance over binary correlation is the fact that this distance measures proximity rather than exact superposition, thus it is more tolerant to perturbations in the locations of points. In addition, since the original definition of the Hausdorff distance is rather sensitive to noise, we opted to use a more robust version of this metric, namely the modified Hausdorff distance [16]. Given the sets S and T of the contour pixels of two shapes (fingers), represented by the sets $S=\{s_1,s_2,\cdots,s_{N_f}\}$, $T=\{t_1,t_2,\cdots,t_{N_t}\}$, where $\{s_i\}$ and $\{t_j\}$ denote contour pixels for $i=1,\cdots,N_s$ and $j=1,\cdots,N_t$, the modified Hausdorff distance [16] is defined as follows:

$$H_{Hausdorff}(S,T)=\max(h(S,T),h(T,S)) \qquad (1)$$

where $h(S,T)=\frac{1}{N_s}\sum_{s\in S}\min_{t\in T}\|s-t\|$ (2)

$$h(T,S)=\frac{1}{N_t}\sum_{t\in T}\min_{s\in S}\|s-t\| \quad (3)$$

$\|s-t\|$ is a norm over the elements of the two sets and obviously the contour pixels (s,t) run over the set of indices $i=1,\cdots,N_s$ and $j=1,\cdots,N_t$. In our case this norm is taken to be the Euclidean distance between the two points.

B. Independent Component Analysis (ICA)

ICA is a technique for extracting statistically independent variables from a mixture of variables. It has been successfully used in many applications to find hidden factors within data to be analysed or decomposing it into the original source signals. In this paper, the ICA is applied on grayscale images to extract and summarize prototypical shape information. ICA assumes that each observed signal $\{x_i(k)\}, k=1,\cdots,K$ is a mixture of a set of N unknown independent source signals l_i, through an unknown mixing matrix A. With x_i and l_i forming the rows of the $N\times K$ matrices X and L, respectively, the following model is obtained:

$$X = AL . \quad (4)$$

The data vectors for the ICA analysis are the lexicographically ordered image pixels. The dimension of these vectors is K (for example, K = 30,720, we used (160× 192) images). ICA aims to find a linear transformation **W** for the inputs that minimizes the statistical dependence between the output components y_i, the latter being estimates of the hypothesized independent sources l_i:

$$\hat{L} = Y = WX \quad (5)$$

In order to find such a transformation **W**, which is also called demixing matrix, the fastICA algorithm [17] was implemented. fastICA maximizes the statistical independence between the output components.

There exists two architectures of ICA [17] : ICA_1 and ICA_2 respectively assume the basis images or their mixing coefficients to be independent. ICA_2 architecture produces global features in the sense that every image feature is influenced by every pixel. Depending on the preference, this makes them either susceptible to occlusions and local distortions, or sensitive to holistic properties. Alternatively, ICA_1 produces spatially localized features that are only influenced by small parts of the image. While the details of ICA are available in [10, 17], for the sake of completeness a brief overview is included here.

ICA_1: Each image available is assumed to be a linear mixture of an unknown set of N statistically independent source images. For this model, normalized images of objects-shapes, 160×192, are raster-scanned to yield data vectors of size 30720. Note that the data matrix **X** will be N×30720 dimensional. This matrix is decomposed into N independent source components $\hat{l}_i$, which will take place along the rows of the output matrix $\hat{L} = WX$. Each row of the mixing matrix **A** (N×N), will contain weighting coefficients specific to a given shape. These weights show the relative contribution of the source object-shapes to synthesize a given object-shape. It follows then that, for the test shape $\mathbf{x}_i$, the i^{th} row of **A** will constitute an N-dimensional feature vector. In this work N is a variable and its value is based on the (shape) database in use. In the recognition stage, assuming that the test set (T) follows the same synthesis model with the same independent components, a normalized test shape $\mathbf{x}_{test}$ (1×30720) is projected onto the set of predetermined basis functions. The resulting vector of projection coefficients are compared by:

$$a_{test} = x_{test}\hat{L}^T\left(\hat{L}\hat{L}^T\right)^{-1}. \quad (6)$$

So the similarity score of a test shape T with the $i-th$ image S_i is obtained using the sum absolute distance:

$$H_{ICA1}(S_i,T)=\sum_{j=1}^{N}\left|a_{i,j}-a_{test,j}\right| \quad (7)$$

In both Hausdorff distance and ICA the image with the minimum distance is considered the shape's match.

ICA_2: In this architecture, the superposition coefficients are assumed to be independent rather than the basis images. Thus, this model assumes each of K pixels of the hand images result from independent mixtures of random variables, that is the "pixel sources". For this purpose, the transpose of the data matrix: X^T is considered. The synthesis of a hand in the data set x_i, from superposition of hand "basis images" as in the columns of the estimated $\hat{A}$ matrix. In the recognition stage, assuming again that test hands follow the same model, they are also size reduced with Rx_{test}^T, and multiplied by the de-mixing matrix $W = A^{-1}$. The resulting coefficient vector of a test hand $\mathbf{x}_{test}$ (K×1), found as $\hat{p}_{test} = WRX^T$, which is then compared with predetermined feature vectors of the training stage. Finally, the individual to be tested is simply recognized as the person i* with the closest feature vector $\hat{p}_{i*}$, where distance is measured in terms of cosine of the angle between them:

$$H_{ICA2}(S_i,T)=\frac{\hat{p}_i \bullet \hat{p}_{test}}{\|\hat{p}_i\|\|\hat{p}_{test}\|} \quad (8)$$

C. Score level fusion of the fingers and the palm

The weighted sum rule has been extensively investigated in the literature and it is the most straightforward fusion strategy at the score level. In this case, the matching scores between pairs of fingers and pairs of palms between query and template hands are combined into a single score using a weighted sum as follow:

$$score(Q,T)=\sum_{i=1}^{6} w_i \times score(Q_i,T_i) \quad (9)$$

where *score* is the similarity measure (e.g., distance) between the query Q and the training data T. Q_i, and T_i represent the *i*-th parts) of the query and training data. In our system, the five parts correspond to the little, ring, middle, index and thumb fingers while the sixth part corresponds to the palm. The parameters w_i are the weights associated with the *i*-th part of the hand which need to satisfy the following constraint:

$$\sum_{i=1}^{6} w_i = 1 \quad (9)$$

This strategy was originally used in [14] which concluded the best combination of weights as follow: w_1 = 0.5/12 (little finger), w_2 = 2.5/12 (ring finger), w_3 = 3.0/12 (middle finger), w_4 = 4.5/12 (index finger), w_5 = 0.5/12 (thumb), and w_6 = 1.0/12 (palm). In this work we used the same weights for the ICP/Hausdorff distance based approach. However, we found that for the ICA the palm image contains feature-rich palmprints and thus the ICA score of the palm becomes more distinctive compared with the ICP/Hausdorff strategy. Therefore, in case of Fusion 2 we emphasise more on the palm and our modified weights are: w_1 = 0.5/13 (little finger), w_2 = 2.5/13 (ring finger), w_3 = 3.0/13 (middle finger), w_4 = 4.5/13 (index finger), w_5 = 0.5/13 (thumb), and w_6 = 2.0/13 (palm).

V. Experimental Results and Analysis

Experiments were conducted on the data sets of the Bogazici University. Our hand database contained 1500 colour images of hands of 500 different persons, three images of each person's right hands. The images were acquired with a HP Scanjet 5300c scanner at 45-dpi resolution; hence, the images measured 383×526 pixels in the preprocessing stage. A detailed description of the datasets is available in [10].

First, our segmentation and pose correction algorithms were applied to normalise the hand, fingers and the palm. Second, the hand recognition experiments, based on normalized hand images were performed on five selected population sizes, namely, population subsets consisting of 20, 50, 100, 200, and 500 individuals. Different population sizes help us perceive the recognition performance with increasing number of individuals. A boosting algorithm was applied so that several different formations of subsets (of sizes of 50, 100, and 500) were created by random choice and their performance scores were averaged. It should be noted that since ICA_2 consistently provided better recognition and verification results compared to ICA_1, in the results section only ICA_2 results are analysed.

Identification results: The identification results are shown in Table 1. We aimed to investigate three different aspects in the recognition rate: effect of fusion, training size, and database size. The first set of experiments were conducted to investigate the performance of shape and appearance based techniques separately and then impact of their fusion (Fusion 3). For instance, as found in Table 1, with 20 persons, Fusion 1 (ICP/Hausdorff distance combination) and Fusion 2 (ICA) respectively produced recognition rate of 99.30% and 99.50% when used individually but performance reached 100% when their fusion strategy Fusion 3 was used.

Table 1: CORRECT IDENTIFICATION PERFORMANCE AS A FUNCTION ENROLLMENT SIZE (DOUBLE TRAINING SET)

	Correct identification percentage				
Enrolment size→	20	50	100	200	500
Fusion 1	99.3	99.1	98.3	97.8	96.2
Fusion 2	99.5	99.2	98.5	98.0	97.8
Fusion 3	100	99.5	98.7	98.5	98.2

Second, we intended to see the effect of training sample size, that is, the impact of multiple independent recordings of the individual's hand. Thus, we ran the recognition experiments with a single training and then with the double training set, both in a round robin fashion. More explicitly, let the three sets of hand images subjects be referred to as the sets A, B, C. In the single set experiments, the ordering of the test and training sets were {(A,B), (B,A), (A,C), (C,A), (B,C), (C,B)}. In other words, set A hands were tested against the training set of set B etc. In the double training set, the ordering of the test and training sets were {(A, BC), (B, AC), (C, AB)}, e.g., hands in the test set A were recognized using hands both in the sets B and C. Finally, the recognition scores were averaged from these training and test set combinations. Table 2 indicates that there is a significant improvement when double training datasets are used instead of one. For instance, with a database of 500 subjects, Fusions 1, 2, and 3 respectively gained 3.2%, 2.58%, and 2.1% in recognition the recognition rate when two training datasets were used instead of one.

Table 2: EFFECT OF TRAINING SET SIZE ON THE IDENTIFICATION PERFORMANCE: THE PERCENT POINT IMPROVEMENT SHOWN BETWEEN THE SINGLE- AND DOUBLE-TRAINING SET

	Correct identification percentage				
Enrolment size→	20	50	100	200	500
Fusion 1	2.1	3.2	3.5	3.8	3.2
Fusion 2	0.8	1.18	1.45	2.32	2.58
Fusion 3	1.2	1.5	1.8	1.98	2.1

Third, we wanted to see the effect of dataset size. Without loss of generality, with the larger dataset, the recognition rate falls. For instance, as shown in Table 1 with Fusion 3, the recognition rates were 100%, 99.5%, 98.7%, and 98.2% respectively for the database size of 20, 50, 100 and 200 subjects.

Verification Results: The next set of experiments were conducted to investigate the verification performance of the proposed technique. In the verification step, the *genuine hands* have to be differentiated from the *impostor hands*. We calculated the distances between the finger/palm shape of the applicant and the finger/palm shapes collected in the database of the subject that s/he claims to be, and then comparing this score against a (small) threshold. If this distance is below the threshold than the claimant is accepted as true; otherwise he is rejected. In the case an impostor presents himself and his distance to the claimed hands is below the threshold, then we have a false acceptance. Conversely, if the distance between the applicant's hand and those registered in the database is above the threshold we have a case of false rejection. Both

false acceptance and false rejection are the failures in the verification process.

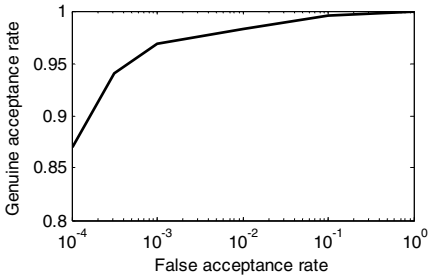

Figure 4: ROC curve for Fusion 3.

In Figure 4 we plot the (lin-log) Receiver Operating Characteristic (ROC) curve for Fusion 3. At 10^{-4} false acceptance rate our algorithm secured the correct acceptance rate of 87%. The verification comparisons between the three feature modalities are given in Table 3 as a function of enrolment size. Notice that for smaller populations (sizes 20, 50, 100, and 200), the performance is calculated as the average of several randomly chosen subject sets.

TABLE 3: VERIFICATION PERFORMANCE AS A FUNCTION OF ENROLLMENT SIZE (EQUAL ERROR RATE)

	Correct verification rate				
Enrolment size→	20	50	100	200	500
Fusion 1	99.9	99.3	98.7	98.2	98.0
Fusion 2	99.7	99.2	98.6	98.1	97.8
Fusion 3	100	99.7	99.4	99.0	98.5

Tables 4 and 5 summarise comparative results (respectively the recognition and verification results) of the proposed algorithm compared with its counterpart proposed in [10]. The reason for selecting this algorithm is twofold: First, it is one of the best shape based hand recognition algorithms available in the literature. Second, it was tested upon the same datasets.

TABLE 4: COMPARISON OF RECOGNITION PERFORMANCE OF ALGORITHMS FOR GIVEN ENROLLMENT SIZES

Enrolment size↓	[10]	Proposed algorithm
20	99.48	100
35	99.40	99.6
70	99.03	99.2
458	97.31	98.25
500	-	98.2

TABLE 5: COMPARISON OF VERIFICATION PERFORMANCE OF ALGORITHMS FOR GIVEN ENROLLMENT SIZES

Enrolment size↓	[10]	Proposed algorithm
20	99.55	100
50	99.40	99.7
100	98.85	99.4
458	98.21	98.55
500	-	98.5

VI. CONCLUSION

We have presented a new approach for hand-based recognition and verification. The proposed system has several advantages over existing methods. It is peg-free, achieves a consistent representation of the fingers and the palm regardless of their pose/orientation or the gaps between the fingers. The proposed algorithm provides better results compared with state of the art algorithms. The superior results are due to the combination of a robust pose invariant hand segmentation algorithm followed by efficient feature extraction and feature matching and fusion techniques.

ACKNOWLEDGMENT

This work was tested on the hand image database provided by Prof Sankur of Bogazici University.

REFERENCES

[1] G. Amayeh, G. Bebis, A. Erol, and M. Nicolescu, "Hand-based verification and identification using palm–finger segmentation and fusion," *Computer Vision and Image Understanding,* vol. 113 pp. 477–501, 2009.

[2] A. Ross and A. K. Jain, "Information fusion in biometrics," *Pattern Recognition Letters,* vol. 24, pp. 2115–2125, 2003.

[3] R. Sanchez-Reillo, C. Sanchez-Avila, and A. Gonzalez-Marcos, "Biometric identification through hand geometry measurements," *IEEE Trans. Pattern Anal. Mach. Intell,* vol. 22, pp. 1168–1171, 2000.

[4] A. K. Jain, A. Ross, and S. Pankanti, "A prototype hand geometry based verification system," presented at the 2nd Int. Conf. Audio- and Video-Based Biometric Person Authentication, 1999.

[5] A. K. Jain, A. Ross, and S. Prabhakar, "Biometrics-BasedWeb Access," 1998.

[6] A. Kumar and D. Zhang, "Personal recognition using hand shape and texture," *IEEE Transactions on Image Processing,* vol. 15, pp. 2454–2461, 2006.

[7] A. Kumar and D. Zhang, "Personal recognition using hand shape and texture," *IEEE Transactions on Image Processing* vol. 15, pp. 2454–2461, 2006.

[8] A. Kumar and D. Zhang, "Personal authentication using multiple palmprint representation," *Pattern Recognition,* vol. 38, pp. 1695 – 1704, 2005.

[9] C. Öden, A. Erçil, and B. Büke, "Combining implicit polynomials and geometric features for hand recognition," *Pattern Recognit. Lett,* vol. 24, pp. 2145–2152, 2003.

[10] E. Yoruk, E. Konukoglu, B. Sankur, and J. Darbon, "Shape-based hand recognition," *IEEE Transactions on Image Processing,* vol. 15, pp. 1803-1815, 2006.

[11] M. Cheung, M. Mak, and S. Kung, "A two level fusion approach to multimodal biometrics verification," presented at the IEEE International Conference on Acoustics, Speech, and Signal Processing (ICASSP'05), 2005.

[12] A. El-Sallam and A. S. Mian, "Human body pose estimation from still images and video Frames " *LNCS,* vol. 6111, pp. 176-188, 2010.

[13] P. J. Besl and N. D. McKay, "A method for registration of 3-D shapes," *IEEE Trans. Pattern Anal. Mach. Intell,* vol. 14, pp. 239–256, 1992.

[14] G. B. G. Amayeh, A. Erol, and M. Nicolescu, "A component-based approach to hand verification," presented at the IEEE Conference on Computer Vision and Pattern Recognition (CVPR '07), 2007.

[15] E. Konukoğlu, E. Y. J., Darbon, and B. Sankur, "Shape-based hand recognition," *IEEE Transactions on Image Processing,* vol. 15, pp. 1803-1815, 2006.

[16] B. Takacs, "Comparing face images using the modified Hausdorff distance," *Pattern Recognition,* vol. 31, pp. 1873-1881, 1998.

[17] A. Hyvarinen and E. Oja, "Independent component analysis: Algorithms and applications," *Neural Networks,* vol. 13, pp. 411-430, 2000.